# Journal of Materials Chemistry A

Accepted Manuscript


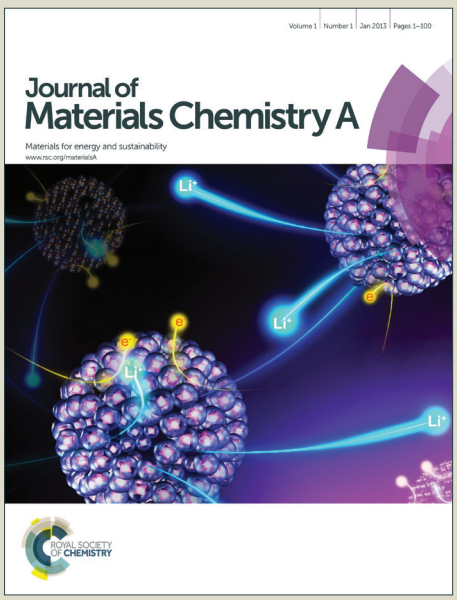





ROYAL SOCIETY OF CHEMISTRY

www.rsc.org/materialsA

Cite this: DOI: 10.1039/c0xx00000x

www.rsc.org/xxxxxx

ARTICLE TYPE

# Ultrathin-Nanosheet-based 3D Hierarchical Porous $In_2S_3$ Microspheres: Chemical Transformation Synthesis, Characterization, and Enhanced Photocatalytic and Photoelectrochemical Property

**Rui Wu[a,b], You Xu[b], Rui Xu[b], Yi Huang[a,b] and Bin Zhang*[b]**

***Received (in XXX, XXX) Xth XXXXXXXXX 200X, Accepted Xth XXXXXXXXX 200X***
**DOI: 10.1039/b000000x**

**Enginnering two-dimensional (2D) ultrathin nanosheets into hierarchical porous structure is one of the important challenges in material chemistry. We report a chemical transformation route to inorganic hierarchical $In_2S_3$ with 3D microsphere-like porous structure stacked by 2D ultrathin nanosheets via an organic-component depletion method of inorganic-organic hybrids as precursors. The as-prepared $In_2S_3$ owns enhanced photocatalytic property for the degradation of methyl orange as well as a stable photoelectrochemical property.**

In the past few decades, microstructured materials with controlled morphology and composition have gained tremendous attention due to their superior applications compared with their bulk counterparts.[1] Among them, 2D ultrathin nanosheets represent an outstanding role because of their excellent unusual physical, chemical and electronic properties, making them promising candidates in fields of catalysis, supercapacitor, batteries and energy device.[2] The exfoliation top-down synthesis has been widely used in the preparation of 2D ultrathin nanosheets. Meanwhile, porous structures have triggered much attention as they can provide large specific surface area as well as more active sites.[3] For instance, the Lou group has built mesoporous $BiVO_4/Bi_2S_3$ heterostructure with enhanced photocatalytic activity toward reduction of $Cr^{4+}$.[3b] However, the hierarchical porous structure stacked by 2D ultrathin nanosheets is hard to reach using reported strategies. Recently, inorganic-organic hybrids,[4] which combine the superior performance of both inorganic building blocks and organic components, have emerged as promising materials as they possess some interesting and unexpected properties. At the same time, they can also act as precursors to be transformed into inorganic materials.[5] On the other hand, since the pioneer efforts by the A. P. Alivisatos group,[6a] nanoscale chemical transformation (e.g. Kirkendall effect, the ion-exchange reaction and stabilizer-depleted method) strategy is becoming more and more popular as one can easily control the structure and chemical composition of products.[6] The utilization of chemical transformation in the further reaction of inorganic-organic hybrids may be a novel, handy but effective strategy to prepare novel inorganic functional materials with good control of components and retention of macro-morphology, which has been little reported.[3c,7] Recently, our group has demonstrated the preparation of inorganic porous single-crystal-like $Cd_xZn_{1-x}S$ nanosheets，hollow $Cd_xZn_{1-x}Se$ nanoframes and porous $MoS_2$ nanotubes through ion-exchange and component stripping strategy of inorganic-organic hybrid precursors, respectively.[7] However, it still remains a big challenge to fulfill the toolbox of this novel and efficient strategy, such as the formation of hierarchical porous structures composed of 2D ultrathin nanosheets.[1e, 1f]

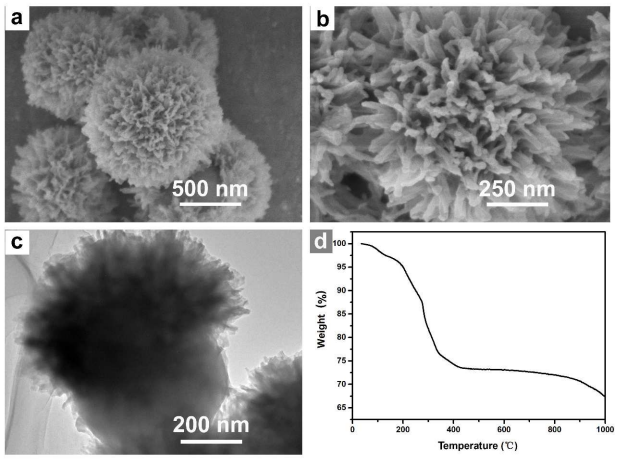


**Figure 1.** SEM images (a, b), TEM image (c) and thermogravimetric analysis curve (d) of InS-TETA precursors.

Due to the consumption of fossil cells and severe environmental problems, it's emergent to explore new energy sources. Among some potential ones, solar energy attracts intensive attentions because of its wide storage and clean feature.[8] Despite the rapid development of photocatalytic materials[9] such as $TiO_2$ and transition metal sulfides, the quick recombination of photo-generated electron-hole pairs and the low transfer rate of electron carriers from inner to surface are still main problems to limit the photocatalytic ability and efficiency. $In_2S_3$, a typical III – VI group chalcogenide with three different structures, $\alpha$-$In_2S_3$, $\beta$-$In_2S_3$ and $\gamma$-$In_2S_3$, is of great interest as an ideal environmentally nontoxic and thermally stable candidate for CdS and CdSe.[10] Among them, the defect spinel structure $\beta$-$In_2S_3$[10a] with a mid band gap (2.0-2.2eV) is an important n-type semiconductor because of its potential use in fields of electrochemistry,[11a,b] photocatalysis,[11c-e] solar cells[11f] and lithium-

ion battery[11g]. Thus, various morphologies including nanowires,[12a] nanobelts,[12b] nanoplates,[12c] nanosheets[12d,e] and nanoflowers[12f,g] have been successfully synthesized by different methods such as oriented attachment,[13a] self-assembly,[13b,c] ligand-assisted method[11c,13d] and atom layer deposition[13e]. However, to the best of our knowledge, 3D hierarchical porous microsphere-like (3HPM) $In_2S_3$ stacked by 2D ultrathin nanosheets have been little reported, especially those prepared by a simple organic-component depletion route.

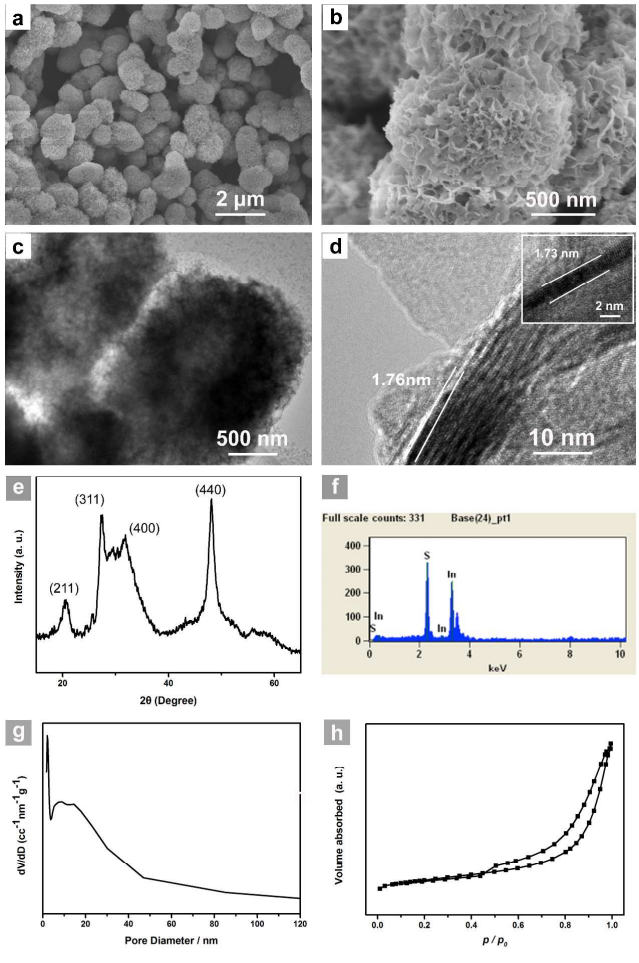


**Figure 2.** SEM (a, b) TEM (c), HRTEM (d) images, XRD patterns (e), energy-dispersed spectrum (f), and pore size distribution (g) and nitrogen adsorption/desorption isotherms (h) of as-converted $In_2S_3$ microspheres stacked by 2D ultrathin nanosheets. Inset in Figure 2d is the TEM image of one typical vertical ultrathin nanosheet.

Herein, we presented a facile synthesis of hierarchical $In_2S_3$ with 3D microsphere-like porous structure stacked by 2D ultrathin nanosheets. An inorganic-organic hybrid (here called InS-TETA, TETA = triethylenetetramine) was used as precursor and continued by using of organic-component depletion method. It has been reported that temperature plays a vital role in the thickness and dispersion of $In_2S_3$, also sufficient amount of amine can help the decomposition of the single source precursor and act as capping ligands, thus deciding the generation of ultrathin $In_2S_3$ nanosheets.[12c,d,e] We further deduced that in the proper temperature and solvent, the little amount of TETA generated by decomposition of InS-TETA hybrids will not only act as capping ligands to facilitate the nucleation of 2D $In_2S_3$ ultrathin nanosheets, but also control the growth of these ultrathin nanosheets with small sizes.[12e] And these small ultrathin nanosheets will selectively grow on microspheres as the required supersaturation here is lower than that in solution,[14] so that the macro-morphology of precursors can be well retained. Thus, we have demonstrated a facile but efficient way to synthesize environmentally friendly 3HPM $In_2S_3$ stacked by 2D ultrathin nanosheets, in which a TETA-solvent-induced nuleation and self-assemble-growth is involved.

First, inorganic-organic InS-TETA precursors were synthesized by the hydrothermal treatment of $InCl_3$, tartaric acid and L-cysteine (see the experimental section in ESI†). As shown in Figure 1a and 1b, the as-synthesized precursors are urchin-like hybrids that consisted of solid spherical inner parts and branch-like outer parts with whole diameter of about 1μm. TEM image further confirms the heterostructure of the as-prepared InS-TETA, while the inner solid sphere has diameter of about 400 nm (Figure 1c). The thermogravimetric analysis (TGA) is continuously used to examine the quality of organic parts contained in the as-prepared InS-TETA (Figure 1d). The TGA image clearly shows two steps of weight loss: the first step is up to 180℃ with a slight weight loss at about 3.5%, which is mainly attributed to the loss of free water and possibly absorbed TETA molecules,[15] and the second step is up to 430℃ with weight loss at about 23.5% due to the loss of TETA molecules in the hybrids. The Fourier transform infrared (FTIR) spectra of products also confirm the existence of TETA in the hybrids (Figure S1†).[15]

When the as-prepared InS-TETA precursors were treated with deionized water (DIW) at 180 ℃ for 10 h, uniformly dispersed 3HPM $In_2S_3$ stacked by 2D ultrathin nanosheets were successfully synthesized. SEM image at low magnification (Figure 2a) reveals 3HPM $In_2S_3$ can be synthesized in large scale, while SEM image at large magnification (Figure 2b) clearly demonstrates its hierarchical porous structure with total diameter of about 1μm, corresponding to that of inorganic-organic hybrid precursors. The detailed structure was then characterized by TEM. The typical TEM image (Figure 2c) of the product reveals a hollow structure, which can result in a much larger specific surface area combined with porous surface, and the magnified TEM images (Figure 2d and Figure S3†) suggest that building blocks of these microspheres are 2D ultrathin layered single-crystalline nanosheets with diameter of about 1.75 nm. XRD patterns of the product (Figure 2e) identify the product as cubic $\beta$-phase that can be indexed to JCPDS no. 00-32-0456.[12d,16] The negligible peak between (311) and (400) can be assigned to (222), which can act as a strong proof of ultrathin $In_2S_3$ nanosheets.[12d] There are no other additional peaks, indicating the high phase purity. And EDX analysis (Figure 2f) further confirms the ingredients of In and S with molar ration of approximately 2:3 without any other impurities, which is corresponding to the result of XRD. To confirm the presence of porous structure, mesopore size distribution was conducted. The Brunauer-Emmett-Teller surface area is calculated to be 90.09 $m^2/g$. Figure 2g suggests the existence of mesopore with size of about 15 nm. The mesopore's nitrogen adsorption/desorption isotherms in Figure 2h can be assigned to a typical IV type isotherm curve, suggesting the existence of mesopores in the as-converted samples. Combined

all these results together, we conclude that InS-TETA hybrid precursor can be successfully transformed into inorganic 3HPM $In_2S_3$ stacked by 2D ultrathin nanosheets via a simple organic-component depletion treatment.

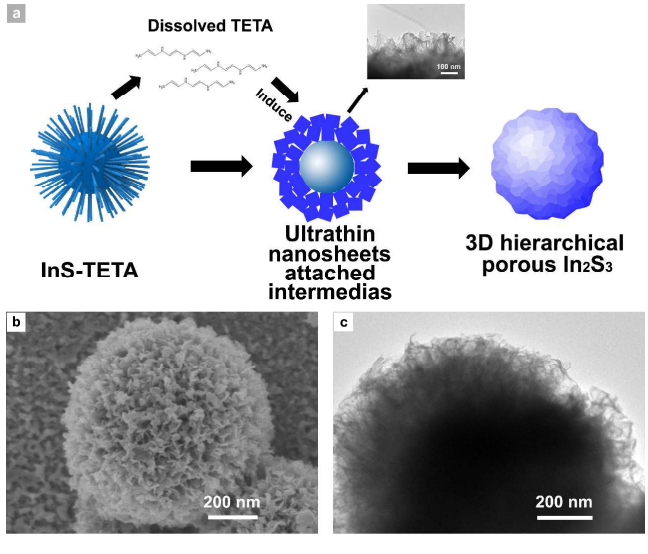


**Figure 3.** (a) Schematic illustration of the evolution mechanism of $In_2S_3$ microspheres stacked by 2D ultrathin nanosheets. Inset is a magnified SEM image of intermediates obtained at 1 h. (b-c) SEM (b) and TEM (c) images of intermediates collected at 1 h.

The detailed mechanism, involving the TETA-solvent-induced nucleation and self-assemble-growth, is confirmed by changing reaction conditions. The whole discussion has two preconditions: the thickness of $In_2S_3$ nanosheets depends on temperature so the ultrathin nanosheets will only be fabricated at 180 ℃,[12d] amine capping ligands are benefit for the formation of 2D ultrathin nanosheets.[12c-e] SEM and TEM images of intermediates at 1 h (Figure 3b, c and Figure S8a†) and 3 h (Figure S8b†) show that at early stage, the precursors may decompose into small nanoparticles. Also, TETA amine molecules dissolve into DIW. These nanoparticle will attach on precursors due to the much lower required supersaturation here and induced by TETA, they generally grow into ultrathin nanosheet building blocks. Meanwhile, the unreacted inner parts will diffuse outward.[7b] Finally, 3HPM $In_2S_3$ stacked by 2D ultrathin nanosheets are achieved (Figure 3a). We then investigate the influence of temperatures, concentrations of starting materials and solvents. First, experiments are conducted under elevated temperature with other conditions unchanged. As shown in Figure S4†, when inorganic-organic hybrid precursors are treated at lower temperature, such as 120 or 150 ℃ (Figure S4a† and Figure S4b†, respectively), microspheres can also be achieved, but the sizes differ from each other evidently and they are not as uniform as which is achieved at 180℃. What's more, products prepared at 120℃ even still contain some organic components, as illustrated by TGA (Figure S2†). When the precursor is treated at 200℃, agglomerate particles composed of several neighboring microspheres are observed instead of mono-dispersed ones (Figure S4c†). We ascribe the differences of these macro-morphologies to the different rate of the dissolution of TETA molecules resulting from elevated temperature, while the building blocks, determined by TETA and solvents (discussed later), remain unchanged. If the rate is too quick (in condition of 200 ℃) or too slow (in condition of 120 ℃ and 150 ℃), the morphology and even the components of products can change easily, showing that the reaction has a relatively high sensitivity to temperature. Second, amine surfactant ligands play a vital role in the floating and dispersion of $In_2S_3$ nanosheets, and insufficient amount will lead to $In_2S_3$ nanosheets with smaller sizes.[12e] So a proper amount of TETA in this system is critical for the nucleation of ultrathin nanosheet building blocks as well as the self-assemble procedure. When the concentration of starting hybrids is diluted (2 mg, Figure S5a†) with other conditions unchanged, microspheres together with some irregular morphologies, such as quasi-cubic and microplates, are clearly observed, possibly caused by the lower amount of TETA generated by lower concentration of starting materials, which has effectively affected the nucleation of $In_2S_3$. If the concentration is enlarged (30 mg, Figure S5b†), highly agglomerate of irregular 3D network-like structure is observed. This is because the high concentration of starting materials can also lead to the large supersaturation, which can raise the rate of reaction and the dissolution of TETA molecules, resulting in excessive agglomerate of nanosheet building blocks. What's more, if the mixture of TETA and DIW is used as solvent instead of pure DIW ($V_{TETA}/V_{DIW}$ = 1/3 with total volume unchanged, Figure S6†), the microsphere-like morphology cannot be also maintained, suggesting the use of pure DIW, or the ratio of TETA to DIW is also essential for the sustainability of macro-sized spherical morphology. This is probably because that the additional amount of TETA will lead to the much fast nucleation, so that the as-prepared $In_2S_3$ nanosheets cannot grow on precursors sufficiently and resulting in the 3D irregular network-like structure. It's worth noting that despite the change of macro-morphology, the building blocks above are prefer to be nanosheets, suggesting that with TETA in DIW, $In_2S_3$ is prefer to nucleate nanosheets initially, and then assemble to various morphologies due to different conditions. But if ethylene glycol (EG) is used as solvent instead of DIW, microspheres, ranging from 0.1μm to 1μm, assembled of nanorods are observed (Figure S7†), which means besides the amount of TETA, the choose of solvents can also adjust the initial nucleation, namely building blocks, of $In_2S_3$, but a self-assemble procedure will always be included in the following growth. And these building blocks are prefer to grow on microspheres as the required supersaturation here is much lower than that in solution, so that the macro-morphology can be maintained. Based on discussions above, we propose a reasonable growth mechanism, the InS-TETA starting materials firstly decompose to generate TETA, and under optimal conditions, the proper amount of TETA act as capping ligands to help fabricate $In_2S_3$ 2D ultrathin nanosheets with a small size closely attached on precursors due to the lower required supersaturation. Finally, the 3HPM $In_2S_3$ stacked by 2D ultrathin nanosheets are fabricated (Figure 3a and Figure S9†).

Recently, the photocatalytic degradation of organic pollutants by semiconductors with solar energy for wasted water purification has triggered much attention. Herein, we reported the photocatalytic property for the degradation of MO of as-prepared $In_2S_3$. MO is a stable azo dye which is widely adopted as a model pollutant to evaluate the photocatalytic activity of different semiconductors. For comparison, we also synthesized 3D solid microsphere-like (3SM) $In_2S_3$ via a similar route except for the procedure of introduction and extraction of organic TETA molecules (seeing ESI† for detailed). It is fully confessed the using of $In_2S_3$ as photocatalysts for the degradation of MO is based on the excitation of $In_2S_3$ instead of direct excitation of MO.[11d] Figure S11† shows the UV-vis absorption spectra of the as-prepared $In_2S_3$. The absorption edge of about 580 nm is

obviously seen, demonstrating the band gap of the product is about 2.14 eV. Also the 3HPM $In_2S_3$ has strong absorption ranging from visible to UV region, suggesting an excellent photocatalytic property. As seen in Figure 4a, more than 80% MO can be degraded in 90 min using 3HPM $In_2S_3$ as photocatalyst under UV-visible irradiation, and the color change of each step during whole procedure is obvious (Figure 4b and Figure S12†), while only less than 40% MO can be degraded in the same time using 3SM $In_2S_3$ as photocatalyst with other conditions unchanged. It's generally known that the apparent rate constant for the photodecomposition of MO can be calculated by this equation: $k = \ln(c_0/c)/t$.[17] Using the information in Figure 4a and 4b, we calculated that the average apparent rate for 3HPM $In_2S_3$ was 0.018 $min^{-1}$, which is 3 times higher than that of 3SM $In_2S_3$, 0.0055 $min^{-1}$. Compared with the morphology and structure of the comparison group (Figure S10†), the hierarchical porous structure composed of ultrathin nanosheets can be mainly contribute to this huge improvement, which will lead to a larger specific surface area and more active sites. Such conditions will result in faster surface separation of photoinduced electrons and holes, and quicker interfacial charge-carrier transfer, which can bring a more efficient reaction for the oxidation of MO.[1d,7a,7b,18, 19]

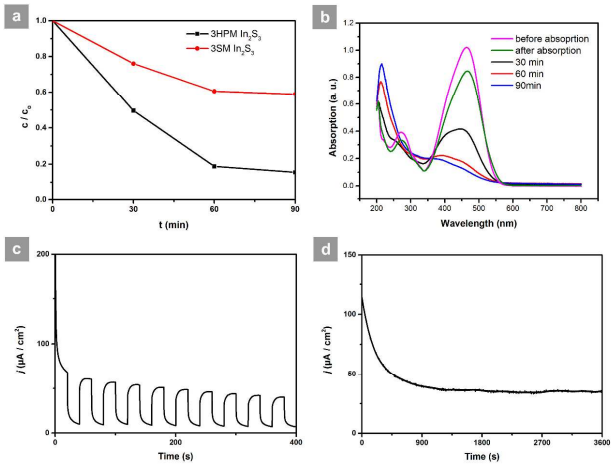


**Figure 4.** Photodegradation of MO over 3D hierarchical porous microsphere-like (3HPM) $In_2S_3$ and 3D solid microsphere-like (3SM) $In_2S_3$ (a). UV/Vis spectral evolution of MO (b) as a function of time under irradiation by using 3HPM $In_2S_3$ as photocatalysts. (c) Photocurrent-density response at an applied bias of 0.8 V versus SCE under UV-visible irradiation of as-converted $In_2S_3$. (d) Photocurrent-time curve for as-converted $In_2S_3$ at static applied potential of 0.8 V versus SCE for 1 h.

Also, we tested the photoelectrochemical (PEC) property of 3HPM $In_2S_3$. Figure 4c shows the photocurrent-density response at an applied bias of 0.8 V versus saturated calomel electrode (SCE) during repeated on/off cycles of UV-visible irradiation in the presence of $H_2SO_4$ (0.5 M). The photocurrent response of 3HPM $In_2S_3$ was prompt, steady and reproducible. Moreover, Figure 4d displayed the photocurrent-time curve at static applied potential of 0.8 V, revealing that 3HPM $In_2S_3$ is highly stable under UV-visible irradiation. Therefore, as-prepared 3HPM $In_2S_3$ could be promising in PEC solar energy conversion devices. We expect that this PEC property can be further enhanced by decorating of graphene or noble metal.[11e]

In summary, we have reported a facile and effective organic-component depletion method to transform inorganic-organic InS-TETA hybrids into 3HPM $In_2S_3$ with single-crystal-like structure stacked by 2D ultrathin nanosheets. The transformation mechanism is discussed in detail, in which a TETA-solvent-induced nucleation and self-assemble-growth is involved. Further investigation shows an improved photocatalytic activity for the degradation of MO, as well as a relatively stable PEC property, which can be attributed to its unique structure and large surface area. What's more, the as-prepared 3HPM $In_2S_3$ may be of great interest as its potential application in fields of solar cells, lithium-ion battery and so on.[11c,f] The facile synthetic strategy may be considered as an important adding toolbox to the chemical transformation of inorganic-organic hybrids, which acts as a novel and promising method to generate inorganic functional materials with good control of structure and chemical components.

The work was financially supported by NSFC (No. 21373149 and No. 21422104).

## Notes and references

[a] *School of Chemical Engineering and Technology, Tianjin University, Tianjin, 300072, P. R. China.*
[b] *Department of Chemistry, School of Science, Tianjin University, and Collaborative Innovation Center of Chemical Science and Engineering (Tianjin), Tianjin, 300072, P. R. China. Fax&Tel: +86 022 2740347; E-mail: bzhang@tju.edu.cn*

† Electronic Supplementary Information (ESI) available: Synthesis of InS-TETA hybrid precursor, 3HPM $In_2S_3$, 3SM $In_2S_3$ and photocatalytic and photoelectrochemical measurement of 3HPM $In_2S_3$, 3SM $In_2S_3$, and Figure S1- S11. See DOI: 10.1039/b000000x/

1 (a) C. H. Cho, C. O. Aspetti, M. E. Turk, J. M. Kikkawa, S. W. Nam and R. Agarwal, *Nat. Mater.*, 2011, **10**, 669; (b) Z. Wang, D. Luan, F. Y. Chiang Boey and X. W. Lou, *J. Am. Chem. Soc.*, 2011, **133**, 4738; (c) S. Chen, S. Z. Qiao, *ACS Nano*, 2013, **7**, 10190; (d) W. Zhou, W. Li, J. Q. Wang, Y. Qu, Y. Yang, Y. Xie, K. F. Zhang, L. Wang, H. G. Fu, D. Y. Zhao, *J. Am. Chem. Soc.*, 2014, **136**, 9280; (e) Y. Li, G. T. Duan, G. Q. Liu and W. P. Cai, *Chem. Soc. Rev.*, 2013, **42**, 3614; (f) Y. Li, N. Koshizaki, H. Q. Wang and Y. Shimizu, *ACS Nano.*, 2011, **5**, 9403.

2 (a) X. Huang, Z. Zeng and H. Zhang, *Chem. Soc. Rev.*, 2013, **42**, 1934; (b) Y. Du, Z. Yin, J. Zhu, X. Huang, X. J. Wu, Z. Zeng, Q. Yan and H. Zhang, *Nat. Commun.*, 2012, **3**, 1177; (c) Y. Sun, Z. Sun, S. Gao, H. Cheng, Q. Liu, J. Piao, T. Yao, C. Wu, S. Hu, S. Wei and Y. Xie, *Nat. Commun.*, 2012, **3**, 1057; (d) J. N. Coleman and M. Lotya, *et al.*, *Science*, 2011, **331**, 568; (e) S. Hu and X. Wang, *Chem. Soc. Rev.*, 2013, **42**, 5577; (f) F. Saleem, Z. C. Zhang, B. Xu, X. B. Xu, P. L. He and X. Wang, *J. Am. Chem. Soc.*, 2013, **135**, 18304.

3 (a) L. Zhang, H. B. Wu, S. Madhavi, H. H. Hug and X. W. Lou, *J. Am. Chem. Soc.*, 2012, **134**, 17388; (b) S. Han, D. Q. Wu, S. Li, F. Zhang and X. L. Feng, *Adv. Mater.*, 2014, **26**, 849; (c) Y. F. Yu, S. X. Hou, M. Meng, X. T. Tao, W. X. Liu, Y. L. Lai and B. Zhang, *J. Mater. Chem.*, 2011, **21**, 10525; (d) Y. Li, W. P. Cai, B. Q. Cao, G. T. Duan, F. Q. Sun, C. C. Li and L. C. Jia, *Nanotech.,* 2006, **17,** 238.

4 (a) X. Y. Huang, J. Li, Y. Zhang and Angelo Mascarenhas, *J. Am. Chem. Soc.*, 2003, **125**, 7049; (b) X. Y. Huang, Harry R. Heulings, V. Le and J. Li, *Chem. Mater.*, 2001, **13**, 3754; (c) M. R. Guo, Y. F. Xu, J. Jiang and S. H. Yu, *Chem. Soc. Rev.*, 2013, **42**, 2986.

5 (a) S. H. Yu and M. Yoshimura, *Adv. Mater.*, 2002, **14**, 296; (b) L. Liao, S. N. Wang, J. J. Xiao, X. J. Bian, Y. H. Zhang, M. D. Scanlon, X. L. Hu, Y. Tang, B. H. Liu and H. H. Girault, *Energy Environ. Sci.*, 2014, **7**, 387; (c) Y. F. Sun, Z. H. Sun, S. Gao, Q. H. Liu, J. Y. Piao, T. Yao, C. Z. Wu, S. L. Hu and Y. Xie, *Nat. Commun.*, 2012, **3**, 1057.

6 (a) D. H. Son, S. M. Hughes, Y. D. Yin and A. P. Alivisatos, *Science*, 2004, **306**, 1009; (b) J. M. Luther, H. M. Zheng, B. Sadtler and A. P. Alivisatos, *J. Am. Chem. Soc.*, 2009, **131**, 16851; (c) U. Y. Jeong, P.

H. C. Camargo, Y. H. Lee and Y. N. Xia, *J. Mater. Chem.*, 2006, **16**, 3893.

7 (a) Y. Yu, J. Zhang, X. Wu, W. Zhao and B. Zhang, *Angew. Chem. Int. Ed.*, 2012, **51**, 897; (b) X. Wu, Y. Fu, Y. Liu, Y. Xu, C. Liu, and B. Zhang, *Angew. Chem. Int. Ed.*, 2012, **51**, 3211; (c) S. Zhuo, Y. Xu, W. Zhao, J. Zhang and B. Zhang, *Angew. Chem. Int. Ed.*, 2013, **52**, 8602.

8 R. G. Li, F. X. Zhang, D. G. Wang, J. X. Yang, M. R. Li, J. Zhu, X. Zhou, H. X. Han and C. Li, *Nat. Commun.*, 2013, **4**, 1432.

9 (a) P. K. Santra and P. V. Kamat, *J. Am. Chem. Soc.*, 2013, **42**, 877; (b) N. Z. Bao, L. M. Shen, T. Takata and K. Domen, *Chem. Mater.*, 2008, **20**, 110; (c) (b) L. Q. Jing, W. Zhou, G. H. Tian and H. G. Fu, *Chem. Soc. Rev.*, 2013, **42**, 9509.

10 (a) W. T. Kim and C. D. Kim, *J. Appl. Phys.*, 1986, **60**, 2631; (b) D. K. Nagesha, X. R. Liang, A. A. Mamedov, G. Gainer, M. A. Eastman, M. Giersig, J. J. Song, T. Ni and N. A. Kotov, *J. Phys. Chem. B*, 2001, **105**, 7490.

11 (a) L. Liu, H. J. Liu, H. Z. Kou, Y. Q. Wang, Z. Zhou, M. M. Ren, M. Ge and X. W. He, *Crys. Growth Des.*, 2009, **9**, 113; (b) Y. Liu, H. Y. Xu and Y. T. Qian, *Crys. Growth Des.*, 2006, **6**, 1304; (c) W. M. Qiu, M. S. Xu, X. Yang, F. Chen, Y. X. Nan, J. L. Zhang, H. Iwai and H. Z. Chen, *J. Mater. Chem.*, 2011, **21**, 13327; (d) Y. H. He, D. Z. Li, G. C. Xiao, W. Chen, Y. B. Chen, M. Sun, H. J. Huang and X. Z. Fu, *J. Phys. Chem. C*, 2009, **113**, 5254; (e) X. Q. An, J. C. Yu, F. Wang, C. H. Li and Y. C. Li, *Appl. Catal. B: Environ.*, 2013, **129**, 80; (f) F. M. Ye, C. Wang, G. H. Du, X. B. Chen, Y. J. Zhong and J. Z. Jiang, *J. Mater. Chem.*, 2011, **21**, 17063.

12 (a) A. Datta, G. Sinha, S. K. Panda and A. Patra, *Crys. Growth Des.*, 2009, **9**, 427; (b) W. M. Du, J. Zhu, S. X. Li and X. F. Qian, *Crys. Growth Des.*, 2008, **8**, 2130; (c) K. H. Park, K. Jang and S. U. Son, *Angew. Chem. Int. Ed.*, 2006, **45**, 4608; (d) S. Acharya, S. Sarkar and N. Pradhan, *J. Phys. Chem. Lett.*, 2012, **3**, 3812; (e) S. Acharya, M. Dutta, S. Sarkar, D. Basak, S. Chakraborty and N. Pradhan, *Chem. Mater.*, 2012, **24**, 1779; (f) L. J. Liu, W. D. Xiang, J. S. Zhong, X. Y. Yang, X. J. Liang, H. T. Liu and W. Cai, *J. Alloys Compd.*, 2010, **493**, 309.

13 (a) Y. H. Kim, J. H. Lee, D. W. Shin, S. M. Park, J. S. Moon, J. G. Nam and J. B. Yoo, *Chem. Commun.*, 2010, **46**, 2292; (b) L. Y. Chen, Z. D. Zhang and W. Z. Wang, *J. Phys. Chem. C*, 2008, **112**, 4117; (c) B. G. Kumar and K. Muralidharan, *J. Mater. Chem.*, 2011, **21**, 11271; (d) S. K. Sarkar, J. Y. Kim, D. N. Goldstein, N. R. Neale, K. Zhu, C. M. Elliott, A. J. Frank and S. M. George, *J. Phys. Chem. C*, 2010, **114**, 8032.

14 D. S. Boyle, K. Govender and P. O'Brien, *Chem. Commun.*, 2002, **38**, 80.

15 Z. A. Zang, H. B. Yao, Y. X. Zhou, W. T. Yao and S. H. Yu, *Chem. Mater.*, 2008, **20**, 4749.

16 M. A. Franzman and R. L. Brutchey, *Chem. Mater.*, 2009, **21**, 1790.

17 Y. Y. Liang, H. L. Wang, H. S. Casalongue, Z. Chen and H. J. Dai, *Nano Res.*, 2010, **3**,701.

18 (a) B. Liu, L. M. Liu, X. F. Lang, H. Y. Wang, X. W. Lou and E. S. Aydil, *Energy & Environ. Sci.*, 2014, **7**, 2592; (b) A.Ivanova, D. F. Rohlfing, B. E. Kayaalo, J. Rathouskỳ and T. Bein, *J. Am. Chem. Soc.*, 2014, **136**, 5930; (c) J. W. Lee, C. Orilall, S. C. Warren, M. Kamperman, F. J. Disalvo and U. Wiesner, *Nat. Mater.*, 2008, **7**, 222.

19 (a) W. J. Zhou, Z. Y. Yin, Y. P. Du, X. Huang, Z. Y. Zeng, Z. X. Fan, H. Liu, J. Y. Wang and H. Zhang, *Small*, 2013, **9**, 140; (b) Y. Xu, W. W. Zhao, R. Xu, Y. M. Shi and B. Zhang, *Chem. Commun.*, 2013, **49**, 9803; (c) M. L. Guan, C. Xiao, J. Zhang, S. J. Fan, R. An, Q. M. Cheng, J. F. Xie, M. Zhou, B. J. Ye and Yi Xie, *J. Am. Chem. Soc.*, 2013, **135**, 10411.

# A Table of Contents Entry

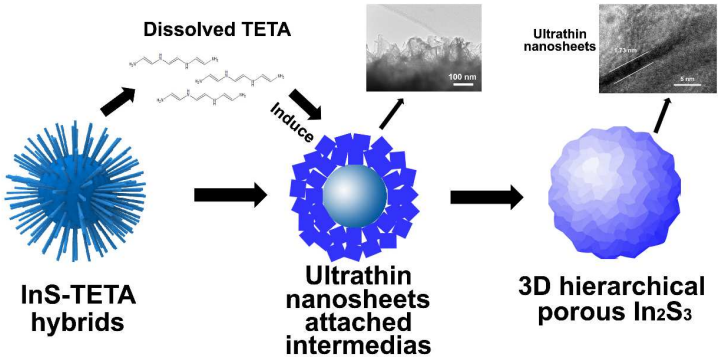


**Ultrathin-nanosheet-based 3D hierarchical $In_2S_3$ with enhanced photocatalytic and photoelectronchemical performance was synthesized via an organic-component depletion method of inorganic-organic hybrids as precursors.**